Radiation Physics and Chemistry 80 (2011) 869–875

Contents lists available at ScienceDirect

Radiation Physics and Chemistry

journal homepage: www.elsevier.com/locate/radphyschem

Influence of 12 MeV electron irradiation on the electrical and photovoltaic properties of Schottky type solar cell based on Carmine

Ş. Aydoğan *, A. Türüt

Atatürk University, Science Faculty, Department of Physics, Erzurum, Turkey

ARTICLE INFO

Article history:
Received 7 October 2010
Accepted 29 March 2011
Available online 6 April 2011

Keywords:
Organic solar cells
Photovoltaic
Ideality factor
Carmine
Electron irradiation

ABSTRACT

A Schottky diode with configuration Au/Carmine/p-Si/Al has been fabricated and it has been seen that the thin film on the p-Si substrate has exhibited a good rectifying behavior. The current–voltage (I–V) characteristics of the device have been investigated in dark before electron irradiation and under white light illumination and after 12 MeV electron irradiation with fluency of 3×10^{12} e^-/cm^2. It has been seen that the device is sensitive to illumination and to electron irradiation. The barrier height value has decreased under illumination. The ideality factor and series resistance values have increased by 12 MeV electron irradiation. Furthermore, it has also seen that the reverse bias current and capacitance of the device have decreased after electron irradiation. This has been attributed to decrease in net ionized dopant concentration with electron irradiation.

1. Introduction

During the last 20 years organic semiconductors have attracted considerable attention due to their interesting physical properties followed by various technological applications in the area of electronics and optoelectronics. One of the main advantages is the fact that they can be produced in large quantities by simple techniques (Stallinga et al., 2002). Besides, their fabrication is simpler and cheaper than that of silicon-based solar cells. Schottky contacts have been extensively used to build various organic electronic devices including organic Schottky diodes (Böhm et al., 2006), organic light-emitting diodes (OLEDs) (Brutting et al., 2001) and organic solar cells (Brabec et al., 2001).

Heterojunction-based semiconductor devices formed by organic compounds grown on inorganic substrates have extensively been investigated by many researchers for their potential use in the electronic and optoelectronic technologies so far. Namely, many devices using organic materials have been fabricated including light-emitting diodes and Schottky-type devices like an inorganic semiconductor/organic semiconductor material or a metal/organic semiconductor material, and their electrical and photoelectrical properties have been investigated for more than three decades. A thin organic layer can easily be made by low cost methods and appropriate processing allows organic thin films to be produced in large areas (Schwoerer and Wolf, 2007; Aydoğan et al., 2008; Farges, 1994; Brabec et al., 1999; Syrrokostas et al., 2009).

In a Schottky barrier the voltage across the metal–semiconductor interface is divided in two contributions: the space-charge region in the semiconductor and the dipole layer in the surface. The dipole layer may consist of a thin oxide layer in inorganic contacts or a double layer in semiconductor–electrolyte contacts. In general the dipole layer is characterized by a constant capacitance (Bisquert et al., 2008; Cowley, 1966; Rhoderick and Williams, 1988).

Until recently the silicon-based photovoltaics (PVs) had advantages in both efficiency and lifetime of the device for monocystalline silicon devices. Organic solar cells have the potential to be competitive on the photovoltaic power market due to expected low production costs even with lower efficiencies and shorter lifetimes compared to their inorganic counterparts (Lungenschmied et al., 2007; Krebs, 2008).

There are a number of operational environments where the performance of materials is likely to be affected significantly by fast-particle irradiation. These include amongst others: fission reactors, proposed fusion reactors, nuclear waste storage containers, particle accelerators and spacecraft. Namely this is not only important for the space community itself but can be beneficial during the process/technology development as well. The reason is that during device or circuit fabrication more and more processing steps use an aggressive environment where irreversible radiation damage can occur. So a fundamental understanding of radiation damage mechanisms and degradation is not only of use for the nuclear/space engineer, but may be helpful for the process engineer as well. In summary, all devices get into touch with each other over the metal/semiconductor contacts in electronic circuits. It is important to determine how the contact parameters of the metal/organic/inorganic semiconductor devices give a response to the

* Corresponding author. Tel.: +90 442 231 4073; fax: +90 442 236 0948.
E-mail address: saydogan@atauni.edu.tr (Ş. Aydoğan).

0969-806X/$ - see front matter © 2011 Elsevier Ltd. All rights reserved.
doi:10.1016/j.radphyschem.2011.03.019

electron irradiation. An understanding of the basic processes involved when materials are exposed to energetic particle irradiation is clearly an important aspect in the choice of materials for use in such environments. There are also cases where irradiation is used as a processing tool, such as ion-beam modification of surfaces and ion-implantation of semiconductors, where again an understanding of fundamental damage mechanisms is of importance. High energy electron studies are used to investigate not only radiation effects themselves, but also the kinetic processes associated with point defects. Electron irradiation is known to have higher damage coefficient than for X-rays and gamma rays (Zoutendyk et al., 1988; Uğurel et al., 2008; Jenkins and Kirk, 2001). It is extremely important to understand the electron irradiation effects on the electrical characteristics of Schottky diodes. The irradiation work on silicon is very important for understanding the behavior of Si devices, which are used in radiation environments like space, nuclear reactors and particle detectors (Summers et al., 1987; Auret et al., 1996). The primary defects in crystals/devices created by energetic electron irradiation are isolated Frenkel pairs of interstitials and vacancies. Most of these point defects have a short life-time and annihilate via the interstitial-vacancy recombination process. The effect of electron irradiation is dependent on the initial or virgin state of the sample. Electron beam techniques such as electron microscopy, electron diffraction methods, electron probe microanalysis (EPMA), Auger electron spectroscopy (AES) and electron energy loss spectroscopy (EELS) widely used in material science at present rely on interaction of the primary electron beam with an analyzed solid (Zemek et al., 2004).

The current–voltage, capacitance voltage and capacitance–frequency characteristics depend on electron irradiation (with 12 MeV and fluency of 3×10^{12} e^-/cm^2) have been investigated. The purpose of this work is to study the electrical characteristics of the Carmine/p-Si Schottky photovoltaic solar cell. The photocurrent characteristics of the device have been also studied under white light illumination.

2. Experimental procedure

A p-type Si semiconductor wafer with (1 0 0) orientation and 400 μm thickness and 1–10 Ω cm resistivity has been used. In order to remove the native oxide and other various contamination on surface on p-Si, the wafer was chemically cleaned using the RCA cleaning procedure (i.e. 10 min boil in $NH_3+H_2O_2+6H_2O$ followed by a 10 min $HCl+H_2O_2+6H_2O$ at 60 °C) before making contacts. The ohmic contact was made by evaporating Al metal on the back of the p-Si substrate, then was annealed at 580 °C for 3 min in N_2 atmosphere. After ohmic contact the native oxide on the front surface of substrate was removed in $HF+10H_2O$ solution. Finally, it was rinsed in de-ionized water for 30 s and was dried. 3 μL of the Carmine organic layer with a thickness of 110 nm was directly formed on the front surface of the p-Si wafer. Then, Au was evaporated on the organic layer at 10^{-5} Torr (diode area$=7.85\times10^{-3}$ cm^2). The molecular formula of the Carmine is $C_{22}H_{20}O_{13}$. Molecular structure is shown in Fig. 1. The current–voltage (I–V) and capacitance–voltage–frequency (C–V–f) measurements of Au/Carmine/p-Si/Al device were performed with KEITHLEY 487 Picoammeter/Voltage Source and HP 4192A (50 Hz–13 MHz) LF IMPEDENCE ANALYZER, respectively.

3. Results and discussion

According to thermionic emission (TE) theory, the current in Schottky barrier diodes (SBDs) can be expressed as (Rhoderick and Williams, 1988):

$$I=I_0\left[\exp\left(\frac{qV}{nkT}\right)-1\right], \tag{1}$$

where

$$I_o=AA^*T^2\ \exp\left(-\frac{q\Phi_b}{kT}\right) \tag{2}$$

is the saturation current. Where Φb is the effective barrier height at zero bias, A^* the Richardson constant and equals to 32 A cm^{-2} K^{-2} for p-type Si, q the electron charge, V the applied voltage, A the diode area, k Boltzmann's constant, T the temperature in Kelvin, n the ideality factor.

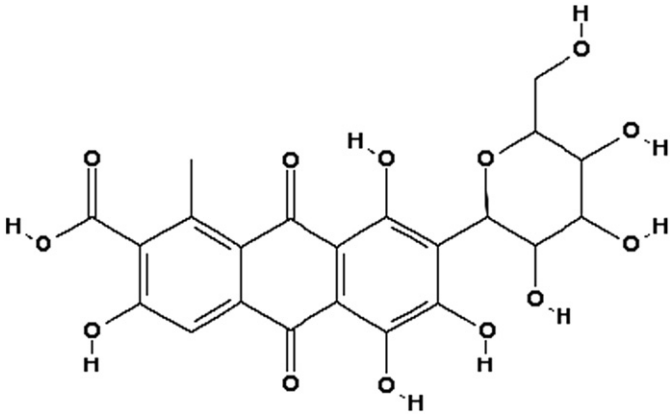

Fig. 1. The molecular structure of the Carmine.

The value of the ideality factor is determined from the slope of the linear region of the forward bias ln I–V characteristic through the relation:

$$n=\frac{q}{kT}\frac{dV}{d(\ln\ I)}. \tag{3}$$

n equals to 1 for an ideal diode. But, it might take a larger value than 1. High values of n can be attributed to the presence of the interfacial thin layer, a wide distribution of low-Schottky barrier height (SBH) patches (or barrier inhomogeneities) and to the bias voltage dependence of the SBH (Rhoderick and Williams, 1988). Φ_b can be obtained from the following equation:

$$\Phi_b=kT/q\ \ln(AA^*T^2/I_0). \tag{4}$$

The current–voltage (log I–V) characteristics of the Au/Carmine/p-Si/Al device depend on electron irradiation and under illumination and in dark (unirradiated) are shown in Fig. 2. It is shown that the device shows a rectifying behavior for each three state. It is clearly seen that the device has been affected by illumination due to the generation–recombination phenomenon. The ratio of forward to reverse current at a given applied voltage is called *rectification ratio*. The rectification ratios are calculated as 1.33×10^3, 0.58×10^3 and 0.25×10^2 at ±0.7 V for in dark (before irradiation), after 12 MeV electron irradiation and under illumination, respectively. The values of the ideality factor and the barrier heights have been calculated and listed in Table 1. It was seen that the device has n value, greater than unity. The higher values of the n may be attributed to either recombination of electrons and holes in the depletion region, inhomogeneities of Carmine film thickness and/or the increase of the diffusion current due to increasing the applied voltage (Yakuphanoglu, 2007). In addition, the barrier height of the Au/p-Si/Al reference device has been calculated as 0.64 eV, which is lower than Au/Carmine /p-Si/Al device. It is clearly seen that Carmine interlayer modifies the effective barrier height by influencing the space

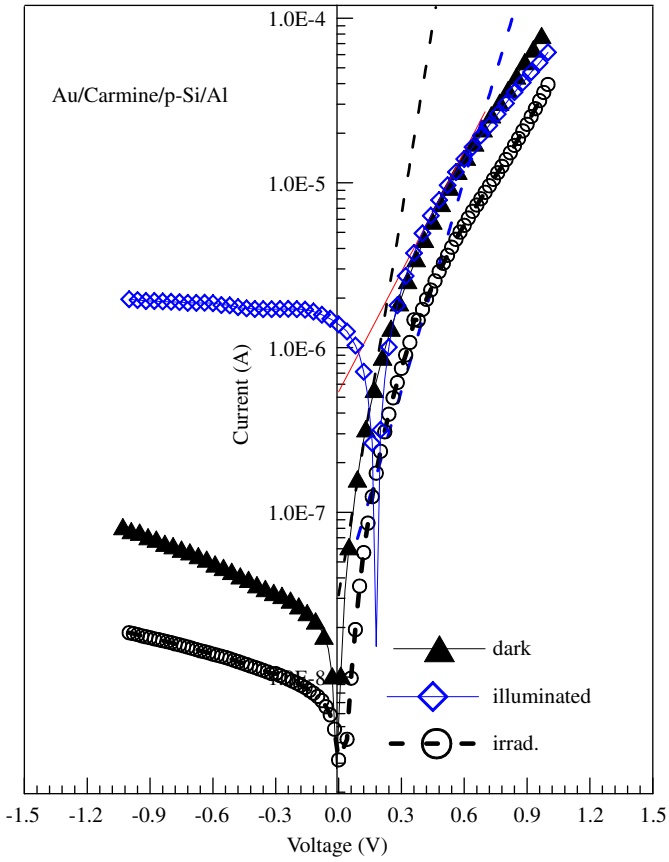

Fig. 2. The current–voltage (log I–V) characteristics of the Au/Carmine/p-Si/Al device.

Table 1
Junction parameters obtained from the I–V characteristics of Au/Carmine/p-Si/Al device.

(a)	n ($I-V$)	Φ_b(eV) (ln $I-V$)	Φ_b(eV) ($H(I)-V$)	Φ_b(eV) ($F(V)-V$)	Φ_b(eV) ($C-V$)
Dark	2.10	0.72	0.82	0.77	0.84
Illumination	4.12	0.62	0.67	0.63	–
Irradiation	3.92	0.71	0.85	0.79	0.83

(b)	$n(d\ln(I)/dV-I)$	$R_S(\Omega)$ $(d\ln(I)/dV-I)$	$R_S(\Omega)$ ($H(I)-I$)	$R_S(\Omega)$ ($F(V)-V$)
Dark	4.35	2080	2087	2146
Illumination	5.88	3390	3400	3396
Irradiation	4.69	2681	2376	2450

charge region of the inorganic silicon substrate. Namely, it is known that this layer forms a physical barrier between the metal and Si substrate, preventing the metal from directly contacting the Si surface.

This result suggests that the transport properties of the device could not be well defined by thermionic emission only. Namely, higher ideality factor could be explained by the secondary transport mechanism at the interface such as tunneling. In addition, it is seen that the I–V characteristics of the device have been affected from the electron irradiation such that the forward bias current value and saturation current have decreased after 12 MeV electron irradiation. This behavior might be attributed to an increase in series resistance, and in interfacial defect density, and to the generation and recombination of the carriers in the depletion layer. Probably, the effects of the defects are more dominated, since the defects can be created in the crystal lattice or the defect concentration might increase after electron irradiation. The irradiation induced defects at the interface might cause tunneling through the barrier and in that case the value of the ideality factor increases (Umana-Membreno et al., 2003).

As a result, the barrier height showed a voltage biasing dependence due to the potential change across the Carmine layer as a result of the applied voltage. Besides, Zahn et al. (2003) have indicated that the initial increase or decrease in effective barrier height for the organic interlayer is correlated with the energy level alignment of the lowest unoccupied molecular orbital with respect to the conduction band minimum of the inorganic semiconductor at the organic–inorganic semiconductor interface.

Fig. 3 shows the I–V characteristics of the device on linear scale, in dark and under white light illumination. It is clearly seen that the device has a photosensitive behavior. At higher forward voltages, the dark and illuminated currents do not differ by appreciable amounts. The reverse bias current of the illuminated device is almost independent of the applied voltage. However, the dark reverse current has smaller than the illuminated curve at all voltages. This situation may be attributed to an increase of the effective mobility and the number of free carriers under illumination. This behavior yields useful information on the electron–hole pairs which has effectively generated in the junction by white illumination. This suggests that the light generates carrier contributing photocurrent due to the production of electron–hole pairs as a result of the light absorption (Farag et al., 2010; Yakuphanoglu et al., 2007).

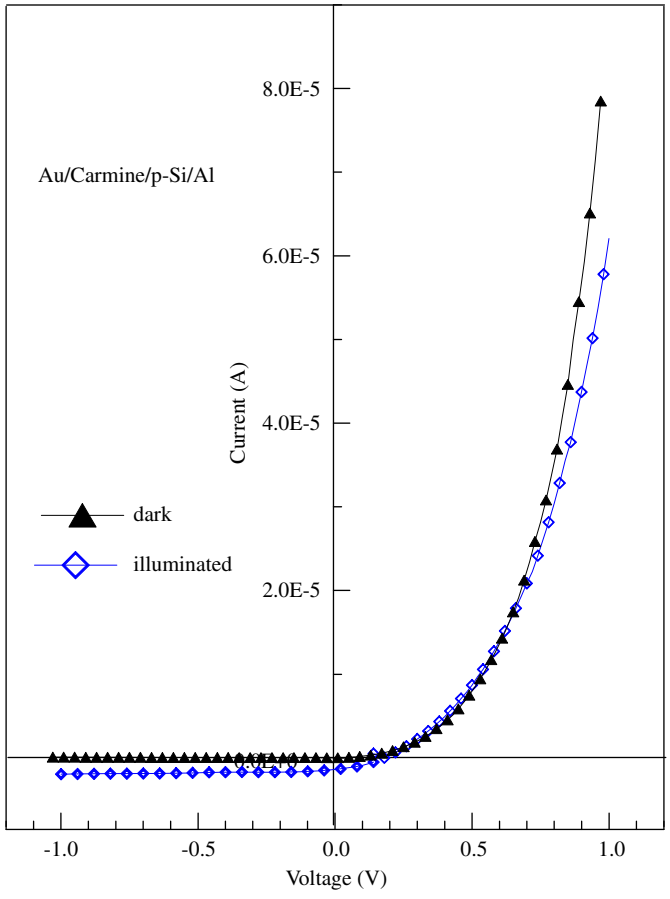

Fig. 3. I–V characteristics of the Au/Carmine/p-Si/Al device in dark and under illumination and after electron irradiation.

The contact parameters of the device are given in Table 1 for under illumination. The value of the ideality factor has been calculated as 4.12 from the *I–V* plots of the illuminated device. Furthermore, the value of the barrier height has been calculated as 0.62 eV due to the increase of the reverse bias current. This result occurs consequently from free charges creation in excess, hence, an increase in the carrier concentration. This effect has a direct influence on the saturation current, the barrier height and the series resistance. The increase in the photocurrent is due to the drift velocity of photogenerated electrons and holes in p-Si.

If a voltage applies on the solar cell, the output current of the illuminated device has two components, the first is the junction current (illumination) due to injection of carriers and the second is the short circuit current due to light generated carriers. As clearly seen in Fig. 2, the reverse current in the dark is small and the diode shows reasonable rectifying characteristics. The currents become 0 at a voltage, called the open circuit voltage V_{OC}=0.21 eV for the *I–V* plots. In the open circuit schema $I(V)=0$ and $I_d(V)=I_d(V_{OC})=I_0\exp(qV_{OC}/kT)$ and it is obtained from Eq.(5),

$$V_{OC}=\frac{kT}{q}\ \ln\ \frac{I_{SC}}{I_0} \tag{5}$$

where I_{SC} is the short circuit current and it has been calculated as 1.05×10^{-4} A. In good solar cells the short circuit current very quickly nears a saturation value. This representation gives information about the fill factor (FF) of the photovoltaic device and therefore gives some essential information about the efficiency of the cell. The fill factor can be calculated according to the following relation (Kar and Varma, 1985):

$$FF=\frac{I_{max}V_{max}}{I_{SC}V_{SC}} \tag{6}$$

The sample shows FF that is equal to 0.24.

The series resistance R_S might affect the performance of the device. Then, the voltage V across the diode can be expressed in term of the total voltage drop V across the series combination of the diode and the resistor. Thus, $V–IR_S$ and for $V>3kT/q$, Eq. (1) becomes

$$I=I_0\ \exp\left[\frac{q(V-IR_s)}{nkT}\right], \tag{7}$$

where the IR_s term is the voltage drop across series resistance of device. The value of the series resistance can be determined from following functions using Eq.(7):

$$\frac{dV}{d(\ln I)}=\frac{nkT}{q}+IR_s \tag{8}$$

$$H(I)=V-\left(\frac{nkT}{q}\right)\ \ln\left(\frac{I}{AA^*T^2}\right), \tag{9}$$

and $H(I)$ is given as follows:

$$H(I)=n\Phi_b+IR_s. \tag{10}$$

Fig. 4 shows the plots of $dV/d(\ln I)$ vs. I of the device. Furthermore, the $H(I)$ vs. I curves are shown in Fig. 5. In addition, based on this equation, the series resistance has been deduced by using the method proposed by Norde (1979).

$$F(V)=\frac{V}{\gamma}-\frac{kT}{q}\ln\left(\frac{I(V)}{AA^*T^2}\right) \tag{11}$$

where γ is an integer (dimensionless) greater than ideality factor, obtained from the *I–V* plots. Fig. 6 shows the $F(V)–V$ plots of the Au/Carmine/p-Si/Al device. Once the minimum of the F vs. V plot is determined, the value of barrier height can be obtained from Eq. (12), where V_0 is the corresponding voltage. The barrier height

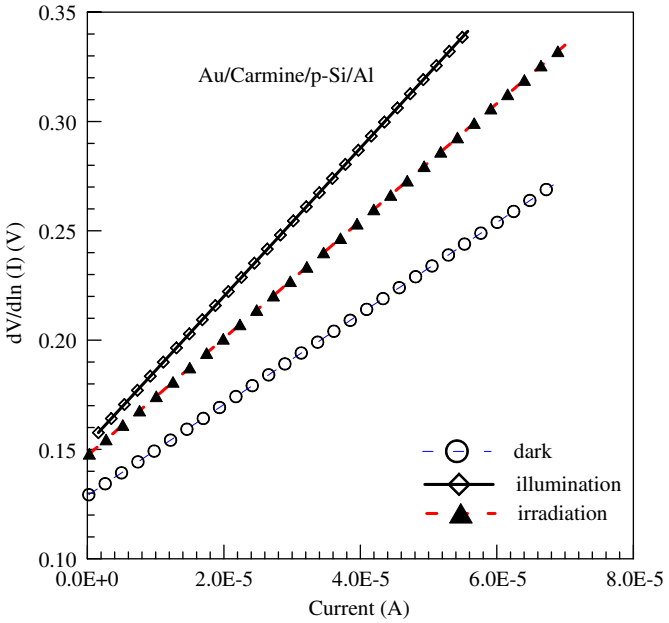

Fig. 4. The plots of $dV/d(\ln I)$ vs. I of the Au/Carmine/p-Si/Al device.

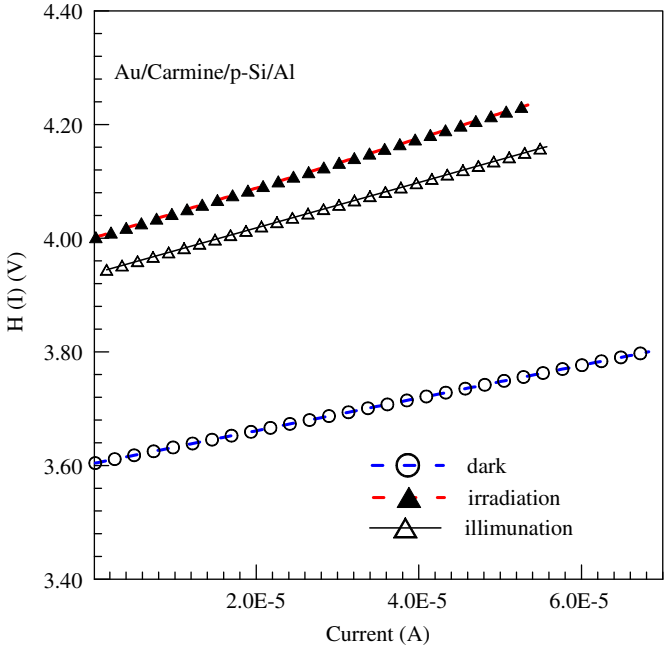

Fig. 5. The $H(I)$ vs. I curves of the Au/Carmine/p-Si/Al device.

is given by Eq. (12) as

$$\Phi_b=F(V)+\frac{V_0}{\gamma}-\frac{kT}{q}. \tag{12}$$

The value of the R_s can be determined by

$$Rs=\frac{kT(\gamma-n)}{qI}. \tag{13}$$

The series resistance values obtained Cheung functions and Norde method are listed in Table 1. It is clearly seen that R_S values have been increased under illumination and after 12 MeV electron irradiation. After irradiation an increase in series resistance indicates that the product of the mobility and the free carrier concentration has reduced. The reduction in mobility is due to the

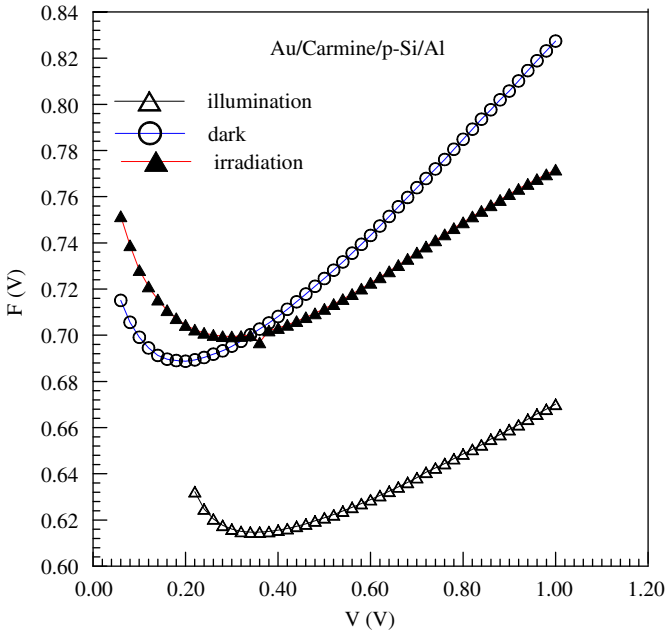

Fig. 6. *F*(*V*)–*V* plot of the Au/Carmine/p-Si/Al.

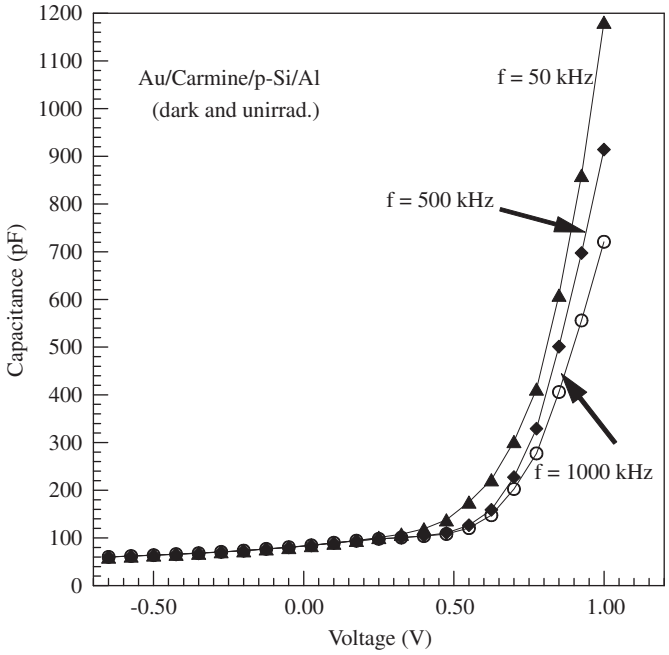

Fig. 7. The *C*–*V* plots of the Au/Carmine/p-Si/Al device in dark , before irradiation, at various frequencies.

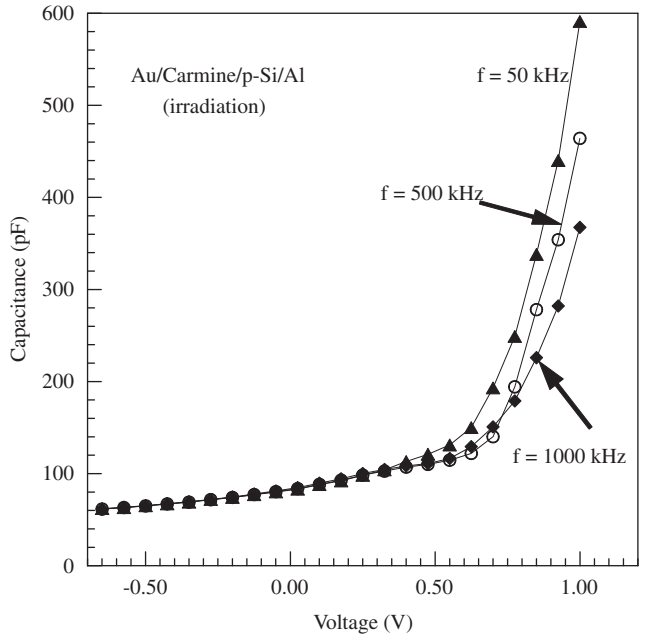

Fig. 8. The *C*–*V* plots of the Au/Carmine/p-Si/Al device after 12 MeV electron irradiation, at various frequencies.

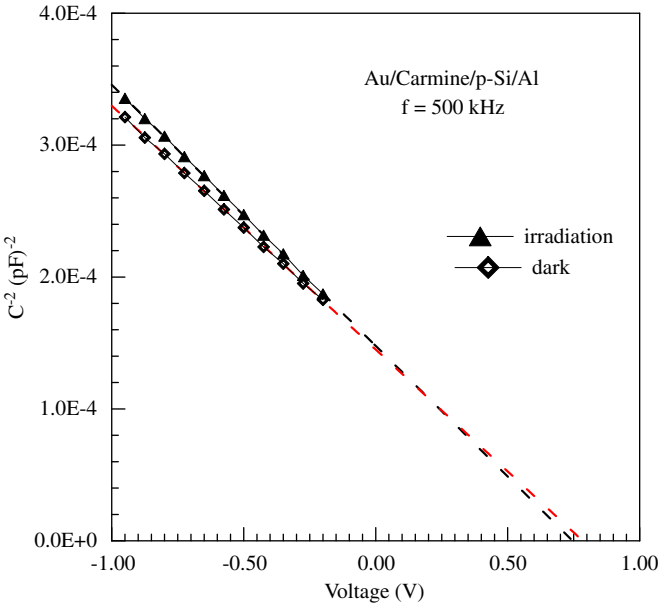

Fig. 9. The reverse bias $1/C^2$–*V* plots of the device for before and after irradiation at $f=500$ kHz frequency.

introduction of defect centers on irradiation which act as scattering centers. The free carrier concentration will be reduced if deep traps are introduced into the material associated with point defect displacement damage. Free carriers in the crystal lattice are captured by the defect centers resulting in decreased carrier density.(Pattabi et al., 2007; Uğurel et al., 2008).

Figs. 7 and 8 show the *C*–*V* plots of Au/Carmine/p-Si/Al device for before irradiation and after 12 MeV electron irradiation, respectively. It is clearly seen from the reverse bias *C*–*V* plots that the value of the capacitance is monotonically increasing towards the higher voltages. In forward bias capacitance is sharply increasing for both states. In addition, it is seen from the figures that the values of the capacitance have been decreased by electron irradiation. This can be attributed to the change in dielectric constant at the interface and/or to decrease in the net ionized dopant concentration with electron irradiation (Güllü et al., 2008; Karatas and Turut, 2006; Zukowski et al.,1997).

The higher values of capacitance at low frequencies are due to the excess capacitance resulting from the interface states in equilibrium with the p-Si which can follow the alternative current (a.c) signal. Namely, the interface states at lower frequencies follow the a.c. signal, whereas at higher frequencies they cannot follow the a.c signal. The values of the capacitance at the high frequency region are only space charge capacitance. Fig. 9 depicts the reverse bias $1/C^2$–*V* plots of the device for before and after irradiation at $f=500$ kHz frequency. Both curves show linear behavior.

From the *C–V* plots, the values of the barrier heights calculated as 0.86 and 0.82 eV at $f=500$ kHz for before and after electron irradiation, respectively. After electron irradiation a small decrease is obtained in barrier height value due to a decrease in diffusion potential. In general, the *C–V* curves gave a Schottky barrier height (BH) value higher than those derived from the *I–V* measurements. This difference can be explained by the different nature of the *C–V* and *I–V* measurement techniques. Besides, barrier heights deduced from the *I–V* and *C–V* techniques are not always the same. If the barriers are uniform and ideal, the two measurements yield the same value; otherwise, they will yield different values. The different behavior of BHs obtained from the two techniques can also be explained by a distribution of BHs due to the inhomogeneties (as a combination of the interfacial oxide layer composition, nonuniformity of the interfacial Carmine layer thickness and distribution of interfacial charges) that occur at interface (Coskun et al., 2004; Werner and Guttler, 1991; Aydoğan et al., 2005).

The capacitance–frequency (*C–f*) characteristics of Au/Carmine/p-Si/Al for unirradiated and after electron irradiation at various voltages are shown in Figs. 10 and 11, respectively. It is clearly seen that the values of the capacitance have decreased after electron irradiation. As described above, this behavior can be attributed to the change in dielectric constant at the interface or to decrease in the net ionized dopant concentration with electron irradiation. In addition, the higher values of capacitance at low frequencies are due to the excess capacitance resulting from the interface states in equilibrium with the p-Si that can follow the a.c signal. The values of the capacitance at the high frequency region originate from only space charge capacitance.

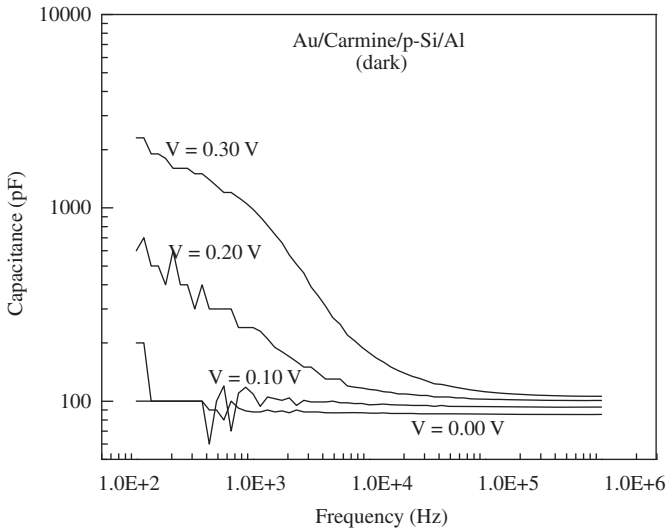

Fig. 10. The capacitance–frequency (*C–f*) characteristics of the Au/Carmine/p-Si/Al for before electron irradiation, at various voltages.

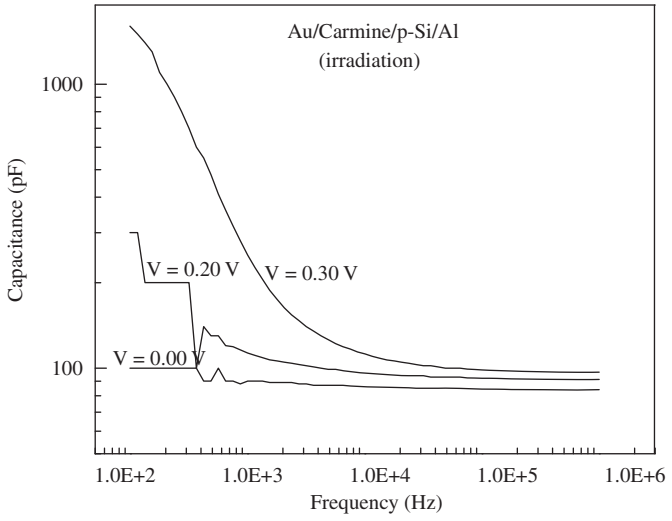

Fig. 11. The capacitance–frequency (*C–f*) characteristics of the Au/Carmine/p-Si/Al for after electron irradiation, at various voltages.

4. Conclusion

It has been found that the electrical characteristics of the Au/Carmine/p-Si/Al device are very sensitive to 12 MeV energy electrons irradiation and to white light illumination. The *I–V* characteristic of the device shows photovoltaic cell-like behavior, under illumination. The device shows photovoltaic behavior with a maximum open-circuit voltage V_{OC} of 0.21 V and a short-circuit current I_{SC} of 1.05×10^{-4} A. This confirms that diode is a promising photodiode. The degradation in the Au/Carmine/p-Si/Al diode properties may be due to the introduction of radiation-induced interfacial defects (between Au and n-Si), and lattice defects via displacement damage.

References

Aydoğan, S., Sağlam, M., Türüt, A., 2005. Current–voltage and capacitance–voltage characteristics of polypyrrole/p-InP structure. Vacuum 77, 269–274.
Aydoğan, S., Güllü, O., Türüt, A., 2008. Fabrication and electrical properties of Al/aniline green/n-Si/AuSb structure. Materials Science in Semiconductor Processing 11 (11), 53.
Auret, F.D., Goodman, S.A., Erasmus, R., Meyer, W.E., Myburg, G., 1996. Electronic and annealing properties of a metastable He-ion implantation induced defect in GaAs. Nuclear Instruments and Methods in Physics Research B 119, 51.
Bisquert, J., Garcia-Belmonte, G., Munar, A., Sessolo, M., Soriano, A., Bolink, H.J., 2008. Band unpinning and photovoltaic model for P3HT:PCBM organic bulk heterojunctions under illumination. Chemical Physics Letters 46, 57–62.
Böhm, M., Ullmann, A., Zipperer, D., Knobloch, A., Glauert, W.H. and Fix, W. 2006. Printable electronics for polymer RFID. In: IEEE ISSCC Dig. Tech. Papers, pp. 270–271.
Brabec, C.J., Padinger, F., Hummelen, J.C., Janssen, R.A.J., Sariciftci, N.S., 1999. Realization of large area flexible fullerene-conjugated polymer photocells: a route to plastic solar cells. Synthetic Metals 102, 861–864.
Brabec, C.J., Sariciftci, N.S., Hummelen, J.C., 2001. Plastic solar cells. Advanced Functional Materials 11, 15–26.
Brutting, W., Berleb, S., Muckl, A.G., 2001. Device physics of organic light-emitting diodes based on molecular materials. Organic Electronics 2, 1–36.
Coskun, C., Aydogan, S., Efeoglu, H., 2004. Temperature dependence of reverse bias capacitance–voltage characteristics of Sn/p-GaTe Schottky diodes. Semiconductor Science and Technology 19, 242.
Cowley, A.M., 1966. Depletion capacitance and diffusion potential of gallium phosphide Schottky-barrier diodes. Journal of Applied Physics 37, 3024.
Farag, A.A.M., Ashery, A., Ahmed, E.M.A., Salem, M.A., 2010. Effect of temperature, illumination and frequency on the electrical characteristics of Cu/p-Si Schottky diode prepared by liquid phase epitaxy. Journal of Alloys and Compounds 495, 116–120.
Farges, J.P. (Ed.), 1994. Organic Conductors: Fundamentals and Applications. Marcel Dekker Inc., New York.
Güllü, O., Aydoğan, Ş., Şerifoğlu, K., Türüt, A., 2008. Electron irradiation effects on the organic-on-inorganic silicon Schottky structure. Nuclear Instruments and Methods in Physics Research A 59, 544–549.
Jenkins, M.L., Kirk, M.A., 2001. Characterisation of Radiation Damage by Transmission Electron Microscopy. Institute of Physics Publishing.
Kar, S., Varma, S., 1985. Determination of silicon-silicon dioxide interface state properties from admittance measurements under illumination. Journal of Applied Physics 58, 4256.
Karatas, S., Turut, A., 2006. Electrical properties of Sn/p-Si (MS) Schottky barrier diodes to be exposed to ^{60}Co γ-ray source. Nuclear Instruments and Methods in Physics Research A 566, 584.
Krebs, F.C., 2008. Air stable polymer photovoltaics based on a process free from vacuum steps and fullerenes. Solar Energy Materials & Solar Cells 92, 715–726.
Lungenschmied, C., Dennler, G., Neugebauer, H., Sariciftci, S.N., Glatthaar, M., Meyer, T., Meyer, A., 2007. Flexible, long-lived, large-area, organic solar cells. Solar Energy Materials & Solar Cells 91, 379–384.
Norde, H., 1979. A modified forward *I-V* plot for Schottky diodes with high series resistance. Journal of Applied Physics 50, 5052.

Pattabi, M., Krishnan, S., Ganesh, S., Mathew, X., 2007. Effect of temperature and electron irradiation on the *I–V* characteristics of Au/CdTe Schottky diodes. Solar Energy 81, 111–116.

Rhoderick, E.H., Williams, R.H., 1988. Metal–Semiconductor Contacts. Clarendon Press, Oxford.

Schwoerer, M., Wolf, H.C., 2007. Organic Molecular Solids. WILEY-VCH Verlag GmbH & Co. KGaA, Weinheim.

Stallinga, P., Gomes, H.L., Murgia, M., Müllen, K., 2002. Interface state mapping in a Schottky barrier of the organic semiconductor terrylene. Organic Electronics 3, 43–51.

Summers, G.P., Burke, E.A., Dale, C.J., Wolicke, E.A., Marshall, P.W., Gehlhausen, M.A., 1987. Comlatim of particle induced diaplacement damage in Si. IEEE Transactions on Nuclear Science 34, 1134.

Syrrokostas, G., Giannouli, M., Yianoulis, P., 2009. Effects of paste storage on the properties of nanostructured thin films for the development of dye-sensitized solar cells. Renewable Energy 34, 1759–1764.

Uğurel, E., Aydoğan, Ş., Şerifoğlu, K., Türüt, A., 2008. Effect of 6 MeV electron irradiation on electrical characteristics of the Au/n–Si/Al Schottky diode. Microelectronic Engineering 85, 2299–2303.

Umana-Membreno, G.A., Dell, J.M., Parish, G., Nener, B.D., Faraone, L., Mishra, U.K., 2003. ^{60}Co gamma irradiation effects on n-GaN Schottky diodes. IEEE Transactions on Electron Devices 50, 2326–2334.

Werner, J.H., Guttler, H.H., 1991. Barrier inhomogeneities at Schottky contacts. Journal of Applied Physics 69, 1522.

Yakuphanoglu, F., 2007. The current–voltage characteristics of FSS/n-Si heterojunction diode under dark and illumination. Physica B 388, 226–229.

Yakuphanoglu, F., Tugluoglu, N., Karadeniz, S., 2007. Space charge-limited conduction in Ag/p-Si Schottky diode. Physica B 392, 188–191.

Zahn, D.R.T., Kampen, T.U., Mendez, H., 2003. Transport gap of organic semiconductors in organic modified Schottky contacts. Applied Surface Science 423, 212.

Zemek, J., Gedeon, O., 2004. Low-energy and low-dose electron irradiation of potassium–lime–silicate glass investigated by XPS. Part II. Chemical bonding. Surface and Interface Analysis 36, 884–887.

Zoutendyk, J.A., Goben, C.A., Berdent, D.F., 1988. Comparison of the degradation effects of heavy ion, electron and Cobalt 60 irradiation in an advanced bipolar process. IEEE Transactions on Nuclear Science 35 (6), 1428–1431.

Zukowski, P., Partyka, J., Wegierek, P., 1997. Effect of ion implantation and annealing on the dielectric properties of silicon. Physica Status Solidi A 159, 509.